# Modeling The Effect of Lateral Inhibition in the Retina on Color Perception

Navneedh Maudgalya
*EECS Department*
*University of California, Berkeley*
Berkeley, United States
navneedhm@berkeley.edu

Rishi Upadhyay
*EECS Department*
*University of California, Berkeley*
Berkeley, United States
rishi.upadhyay@berkeley.edu

Nithin Raghavan
*EECS Department*
*University of California, Berkeley*
Berkeley, United States
rnithin@berkeley.edu

***Abstract*—We extend a mathematical model illustrating the effects of retinal fixational drift motion on color perception and shape reconstruction. By taking into account the lateral inhibition of the H1 cell network and properties of the retinal cone mosaic, we are able to create a biologically-plausible model for estimating the retina position and spatio-chromatic information of a natural visual stimulus. Results suggest that a model taking into account lateral inhibition is better able to reconstruct higher-contrast regions of the image, and could potentially show more improvement with a well-chosen dictionary prior.**

***Index Terms*—fixational drift, horizontal cells, eye movement, lateral inhibition, sparse coding**

## I. Introduction

Although human visual perception is incredibly rich and informative, work is still being done to understand how underlying biological mechanisms in the early visual pathway enable rich and coherent percepts. Light is first projected onto the cones in the retinal cone mosaic where three types of cones, each responding with varying sensitivities to light of different wavelengths, process and relay this information to downstream regions in the retina and the visual cortex. Imaging experiments performed with adaptive optics have shown that retinal cone mosaics contain a non-uniform distribution of cone types, random spatial arrangement of cones, and varying cone densities, [3], [4], [17]. To alleviate the negative effects of these attributes, fixational retinal drift motion has been proposed as a mechanism through which inhomogeneities in the retina can be smoothed out by sharing input information across the retina [1], [4].

### A. Role of Retinal Fixational Drift Motion

During visual fixation the human eye makes microscopic movements, continuously altering the retinal projection of the visual stimuli and photoreceptor cell responses. Despite this motion, humans maintain a stable and high-acuity percept of the stimuli. Earlier work described how this eye movement was a hindrance and further neural computation was necessary to remove the blurring effect caused by this motion [10]. However, more recent experiments done by Ratnam, et al. [4], which indicated that humans were more likely to correctly identify the orientation of a moving stimulus than of a stationary stimulus, concluded that the visual system is able to construct higher-resolution percepts by incorporating information about the eye's movement. To corroborate the experimental results demonstrating the utility of retinal motion, Anderson, et al. [1] proposed a mathematical model to explain the neural mechanisms that utilize retinal movement to provide high-acuity vision by jointly estimating the stimuli shape and position of the retina.

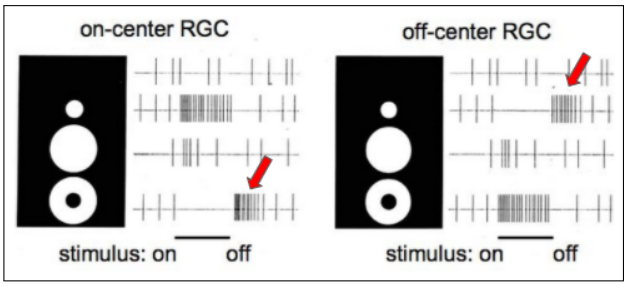


Fig. 1. An illustration of the center-surround receptive fields of midget retinal ganglion cells [18]. Stimulation of the center and lack of stimulation in the surround of an ON cell's receptive field results in an increase in the firing rate of the ganglion cell. Moderate firing response in retinal ganglion cells occur when both the center and surround are stimulated.

### B. Horizontal Cell-Mediated Lateral Inhibition

However, the interactions between retinal motion and horizontal cells in the retina remain unclear. Horizontal cells are found across the cone mosaic and connect neighboring cones and rods to each other using gap junctions. These connections enable inhibitory feedback from neighboring rods and cones to modulate the signal sent to the ganglion cells. These signals emphasize the edges of the input image and remove redundancies between nearby photoreceptor cell responses, whitening the visual stimuli [12]. This inhibitory feedback is called lateral inhibition, which creates the center-surround receptive field in midget ganglion cells (see Fig. 1) [16]. The behavior of horizontal cells has also been used to explain color perception. [11] proposed that interactions between S-cone signals and L versus M-cone signals are responsible for perceiving distinct hues. However, the random spatial arrangement of cones makes it implausible for specific interactions between cone signals to occur across all locations in a static retina to provide high quality color vision. Further work is needed to understand how lateral inhibition affects

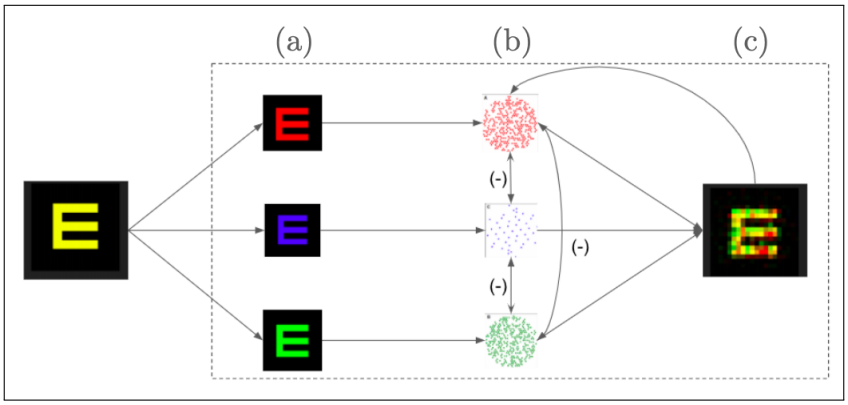


Fig. 2. An overview of our proposed model. (a) The input natural image, in RGB space, split into R, G, and B channels. (b) Using the methodology of [1] we measure the retinal ganglion cell activations for all color channels, taking into account lateral inhibition. (c) Finally, taking into account the activations across all color channels at once, we iteratively alternate between inferring the retina position and the shape and color to reconstruct the original image.

color perception, especially when taking retinal fixational drift motion into account.

### C. Previous Models

The models we extended were created by Anderson, et al. and Sabnis, et al [1], [5]. [1] created the first mechanism for reconstructing a high quality greyscale image by using a joint online expectation maximization (EM) algorithm. The model uses spike data generated by an array of retinal ganglion cells in response to the visual input and the estimated eye position, to infer the input's shape. This updated shape estimate and new spike data generated in response to eye movement is used to re-estimate the position of the eye. The model alternates between these two steps to improve the inference. [5] extended [1] to work with colored images by assigning each L, M and S-cone to the R, G and B channels of an image representing an input natural stimulus. To infer the shape of the visual input, they ran the EM model on all three channels independently and concatenated the result. Neither model accounted for the effects of lateral inhibition.

### D. Objectives

**We hypothesize that the nature of lateral inhibition indicates that it will aid in the reconstruction of high-frequency color changes and contours, while reconstructing solid or flat colors somewhat poorly.** To test this, we build off the work done in previous models to produce a more biologically plausible variant to directly infer spatiochromatic information in the presence of retinal fixational drift motion. First, we explain how we adapted the Anderson et al. model to work with colored stimuli. Then, we describe how lateral inhibition was added to the model and share experimental results using natural images that show the joint effect of lateral inhibition and retinal fixational drift motion on perception. Finally, we discuss experiments with different spatio-chromatic priors used for shape and color inference. See Fig. 2 for reference.

## II. Methodology

### A. Updating Prior Model for Colored Input

In order for our model to work with colored images and infer the stimuli's shape by jointly using information across all three color channels, we changed the retinal ganglion cell spiking model. We replaced the homogeneous rectangular cone lattice with a biologically plausible hexagonal cone lattice consisting of three different types of cones randomly arranged and responsive to different color channels. Each cone was connected to an ON and OFF retinal ganglion cell so that these cells only activated in response to input from a certain cone type. The spike trains of all retinal ganglion cells were used to predict the position of the eye and infer the stimuli's shape and the movement of the eye was simulated by translating all cones the same amount.

### B. Updating the Retinal Sampling Lattice

The size and density of this hexagonal lattice are parameters to the model, and all experiments were done with lattices enclosed within a circle of radius 7-15 pixels with a minimum separation of 0.5-1.2 pixels between cones. We used lattices with 45% L, 45% M and 10% S cones. Adjusting these parameters could allow for future exploration of how varying L:M cone ratios can affect lateral inhibition effects.

### C. Adding lateral inhibition

Prior models compute the activation $c$ and the firing rate, $\lambda$, of RGC $j$ at time $t$ using the following equations [1]:

$$c_{j,t} = g \cdot \sum_i S_i T(X_t^R)_{i,j}$$

$$c'_{j,t} = c_{j,t} \text{ if } j \in \text{ON or } 1 - c_{j,t} \text{ if } j \in \text{OFF}$$

$$\lambda_j(S, X_t) = \exp\left(\log \lambda_0 + \log\left(\lambda_1/\lambda_0\right) \cdot c'_{j,t}\right)$$

where $S_i$ is a pixel of the stimuli, $X_t^R$ is the retinal location, and $T(X_t^R)_{i,j}$ is a weighting factor based on the distance between the RGC and the pixel. $\lambda_0$ and $\lambda_1$ are pre-set

minimum and maximum firing frequencies and $g$ is a gain set such that $c_{j,t}$ has a maximum value of 1.

In order to add lateral inhibition, we add an extra term to the first equation so that it becomes:

$$c_{j,t} = g \cdot \max\left(\sum_i S_i T(X_t^R)_{i,j} - q \cdot \sum_{k \in \mathcal{N}} c_{k,t} I(j,k), 0\right)$$

The new term is a weighted sum of the RGC's neighbors where the weighting function $I(j,k)$ is a Gaussian as described in [13] and [14]:

$$I(j,k) = \frac{1}{\sigma\sqrt{2\pi}} e^{-\frac{1}{2}\left(\frac{||X_j - X_k||}{\sigma}\right)^2}$$

The variance of this function, $\sigma$ is a parameter to the model. We restrict $c_{j,t}$ to non-negative values to avoid firing frequencies below the minimum frequency and include a scaling factor $q$. Together, $\sigma$ and $q$ control the strength and extent of the lateral inhibition effect in our model.

For this work we modeled only the H1 horizontal cells which ignore S cones, so when constructing the neighbors set $\mathcal{N}$ for each RGC, we only considered L and M type cones [15].

### D. Model Parameters

As formulated, our model includes four parameters that can be changed to tweak the performance: $\lambda_0, \lambda_1, \sigma$ and $q$. $\lambda_0$ and $\lambda_1$, the baseline and maximum firing rates, were set to 10 Hz and 100 Hz respectively as in [1]. After experimentation, we chose values of 1.75 for $\sigma$ and 0.75 for $q$.

## III. Experiments with Spatio-Chromatic Priors

As in [1], we impose a diffusive random walk as a prior on the eye trajectory. However, we look to incorporate different priors on the stimulus pattern that allow for the simultaneous inference of both shape and color. We follow the example of [1] and incorporate a prior of the form

$$\log p(S|A) = \delta(S - DA)$$

where $S$ is the shape, $D$ is a dictionary matrix and $A$ is the vector of latent codes. For the lateral inhibition experiments, we use the independent pixel prior, which samples $A$ uniformly and lets $D = I$. We considered two ways to generate spatio-chromatic priors, sparse coding with ICA and LCA, and compared these with results obtained using the independent pixel prior (see Fig. 3).

### A. Sparse Coding with ICA

For one experiment, we performed independent component analysis (ICA) to obtain a sparse coding basis. Assume we have the generative model [2]:

$$S = DA + \epsilon$$

where $\epsilon$ is a noise term. We whiten the input shape $S$ to get $\hat{S}$ so that the impact of $\epsilon$ is reduced. To obtain an orthogonal basis for ICA [9], let $D$ represent the list of ICA basis vectors, and obtain the latent factors using the Moore-Penrose pseudoinverse as

$$D^+ \hat{S} = A$$

However, since an overcomplete basis would work better than an orthogonal one, we use the FastICA algorithm [7] to compute the independent component matrix, obtaining the dictionary $D$ and latent code $A$ through gradient descent.

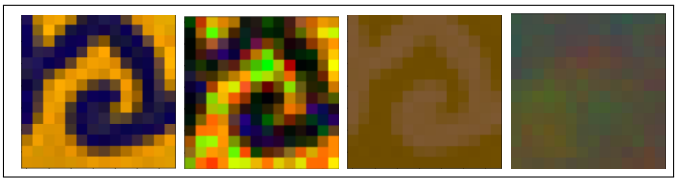

Fig. 3. Experimental results using different priors. From left to right: the original, natural image; reconstruction with an independent pixel prior; reconstruction with the locally competitive algorithm and learning rule; reconstruction with independent component analysis.

### B. Sparse Coding with LCA

For the other experiment, we used the locally competitive algorithm (LCA) with a learning rule to obtain a sparse coding basis. Consider a similar representation of the generative formulation:

$$S(x,y) = \sum_i A_i D_i(x,y) + \epsilon$$

LCA is a biologically plausible method for sparse coding, which attempts to minimize the following function of $S$, $D$, $A$ and a cost function $C$:

$$E(S, A; D) = \frac{1}{2}\left(\sum_{x,y} S_{x,y} - \sum_i A_i D_i(x,y)\right)^2 + \lambda \sum_i C(A_i)$$

The above is also called an energy function. [8] describes the following method for obtaining the optimal $D^*$ and $A^*$, which is done by alternating between using LCA to find the optimal $A^*$ and using the gradient descent learning rule to find the optimal dictionary.

For ICA, our results indicate that while some color and a very weak outline of the input shape is reconstructed, the sparse coding basis was not spatiochromatically optimized for our use case. We believe that future work must be undertaken in order to identify the pre-processing and post-processing techniques (in addition to centering and whitening) that might result in a more accurate reconstruction. For LCA and the learning rule, our results indicate that while a very accurate input shape is reconstructed, the color is not. The code for LCA with gradient descent was based off of an implementation for greyscale (2D) images, which is a potential reason for why the color was not accurately reproduced (we reshaped the 3D image to be 2D, which might not be enough to accurately reproduce spatiochromatic information).

TABLE I
SNR WITH AND WITHOUT LATERAL INHIBITION

| Image | Lateral Inhibition | No Inhibition |
|---|---|---|
| Oski | **5.724 ±0.92** | 5.032 ±1.31 |
| Balls | 3.739 ±0.48 | **4.333 ±0.44** |
| Fire Truck | **3.946 ±0.74** | 3.818 ±0.86 |
| Solid Red | 8.000 ±0.938 | **8.577 ±1.427** |

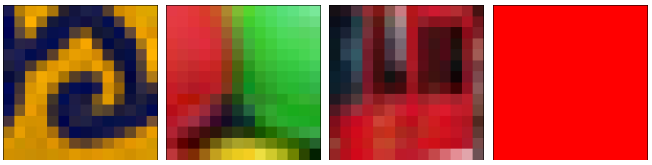

Fig. 4. The ground truth stimuli used to compare the model with and without lateral inhibition. From left to right: Oski, Balls, Fire Truck, and Solid Red.

## IV. Results

In order to test the effects of lateral inhibition on our model, we reconstructed various natural stimuli and solid color stimuli both with and without lateral inhibition. We chose three test images and a red solid color stimuli which are shown in Fig. 4. In order to compare these images, we ran 10 iterations of each reconstruction where the trajectory of the eye movement changed in each iteration. Table 1 contains this data. The model with lateral inhibition performed better on the Oski and Fire Truck images but performed worse on the Balls image and the solid red stimuli. Both the balls image and red stimuli include significant regions of solid color, meaning our results are in line with our hypothesis that lateral inhibition would perform poorly on solid colors while excelling at more high-frequency images.

Overall, it is somewhat difficult to evaluate the effectiveness of lateral inhibition from looking at the SNR of entire images. Hence, we generated error plots for both reconstructions. In order to generate these error plots, we computed the difference between the reconstruction and ground truth in the R, G, and B channels separately, then added them together and averaged across all reconstructions.

Fig. 5 shows an example of these error plots. Combined, the reconstructions and error plots provide some insight into the effect of lateral inhibition: The edges in the image are reconstructed with higher fidelity with lateral inhibition than without. In particular, the reconstruction without lateral inhibition includes significant blurring and discoloration between the red and yellow balls in the bottom left corner. In addition, the error plots show that the reconstructions with lateral inhibition had less error throughout the center of the image where various balls meet.

The independent pixel prior limits the quality of the reconstruction, as this prior does not take into account more widespread color information in an image and produces patchy reconstructions. Furthermore, this prior makes it difficult for the model to reconstruct non-primary colors.

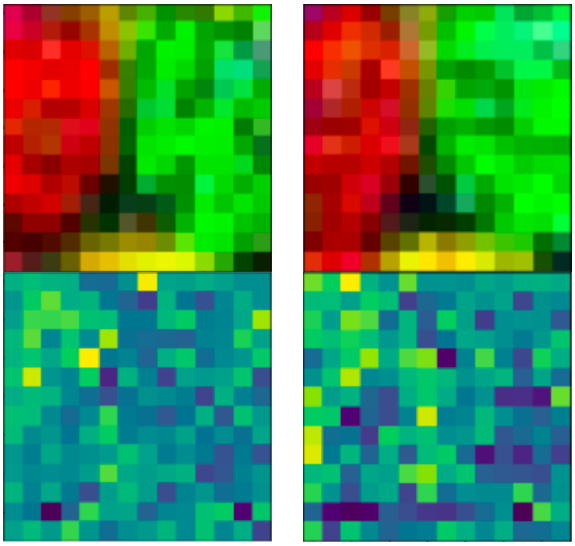

Fig. 5. Analysis of reconstructions of the Balls image. Left: With lateral inhibition, Right: Without lateral inhibition

## V. Discussion

Although our results suggest that lateral inhibition aids in perceiving high-contrast areas of natural visual stimuli, the reconstructions using lateral inhibition and those not using lateral inhibition are perceptually quite similar. Further experiments are necessary to first understand the direct effect of lateral inhibition on RGC activations, prior to shape inference. These experiments should use fewer cones in the sampling lattice and simpler visual stimuli to better understand how and when lateral inhibition improves our perception. It may even be useful to design separate experiments to understand how lateral inhibition affects color and shape perception independently.

Due to the limitations of the independent pixel prior, further research should be done to construct a spatio-chromatic prior that takes into account global color information in the image to effectively utilize all RGC activations when reconstructing the original image.

Additionally, the temporal effects of lateral inhibition (see Fig. 1) could also be implemented to achieve a more accurate result and experiments could be run to understand how the fidelity of the shape and color reconstruction deteriorates as cone density is reduced.

## VI. Acknowledgements

We'd like to thank Alex Anderson, Kaylo Littlejohn, Arjun Sabnis, Jesse Ku, Hugh Johnson, Bruno Olshausen, Ren Ng, Weili Liu, Yin Tang and Frank Cai for their help.

## References

[1] Alexander G. Anderson, Kavitha Ratnam, Austin Roorda, Bruno A. Olshausen; High-acuity vision from retinal image motion. Journal of Vision 2020;20(7):34. doi: https://doi.org/10.1167/jov.20.7.34.

[2] Olshausen, B. A. (2008). Sparse Coding and 'ICA'.

[3] Chui TY, Song H, Burns SA. Adaptive-optics imaging of human cone photoreceptor distribution. J Opt Soc Am A Opt Image Sci Vis. 2008;25(12):3021-3029. doi:10.1364/josaa.25.003021

[4] Kavitha Ratnam, Niklas Domdei, Wolf M. Harmening, Austin Roorda; Benefits of retinal image motion at the limits of spatial vision. Journal of Vision 2017;17(1):30. doi: https://doi.org/10.1167/17.1.30.

[5] Arjun Sabnis, Jesse Ku, Hugh Johnson; Generation of Stable Color Perception from Fixational Retinal Drift. In *Computer Science 294-164*, 2019.

[6] Fairchild, Mark D. (2005). Color Appearance Models (2E ed.). Wiley Interscience. pp. 182–183, 227–230. ISBN 978-0-470-01216-1.

[7] Hyvärinen, A.; Oja, E. (2000). "Independent component analysis: Algorithms and applications" (PDF). Neural Networks. 13 (4–5): 411–430. CiteSeerX 10.1.1.79.7003. doi:10.1016/S0893-6080(00)00026-5. PMID 10946390.

[8] Olshausen, B. A. (2018). Sparse coding via a locally competitive algorithm (LCA).

[9] Mark S. Drew and Steven Bergner. 2008. Spatio-chromatic decorrelation for color image compression. Image Commun. 23, 8 (September, 2008), 599–609. DOI:https://doi.org/10.1016/j.image.2008.05.006

[10] Yoram Burak, Uri Rokni, Markus Meister, Haim Sompolinsky. Bayesian model of dynamic image stabilization in the visual system. Proceedings of the National Academy of Sciences. Nov 2010, 107 (45) 19525-19530; DOI: 10.1073/pnas.1006076107.

[11] Brian P. Schmidt, Maureen Neitz, and Jay Neitz, "Neurobiological hypothesis of color appearance and hue perception," J. Opt. Soc. Am. A 31, A195-A207 (2014)

[12] Graham DJ, Chandler DM, Field DJ. Can the theory of "whitening" explain the center-surround properties of retinal ganglion cell receptive fields?. Vision Res. 2006;46(18):2901-2913. doi:10.1016/j.visres.2006.03.008

[13] Rodieck RW, Stone J. Analysis of receptive fields of cat retinal ganglion cells. J Neurophysiol. 1965;28:832–849. PMID:5867882

[14] Shapley R, Enroth-Cugell C. Visual adaptation and retinal gain controls. Prog Retin Eye Res. 1984;3:263–346.

[15] D.M. Dacey, B.B. Lee, D.K. Stafford, J. Pokorny, and V.C. Smith, Horizontal cells of the primate retina: cone specificity without spectral opponency. Science 1996;271:656–659

[16] Masland RH. The neuronal organization of the retina. Neuron. 2012 Oct 18;76(2):266-80. doi: 10.1016/j.neuron.2012.10.002. Epub 2012 Oct 17. PMID: 23083731; PMCID: PMC3714606.

[17] Legras R, Gaudric A, Woog K (2018) Distribution of cone density, spacing and arrangement in adult healthy retinas with adaptive optics flood illumination. PLOS ONE 13(1): e0191141. https://doi.org/10.1371/journal.pone.0191141

[18] Heeger, D. (2020). Perception Lecture Notes: Retinal Ganglion Cells. Retrieved December 09, 2020, from http://www.cns.nyu.edu/ david/courses/perception/lecturenotes/ganglion/ganglion.html